

A sol–gel derived $\text{CuO}_x/\text{Al}_2\text{O}_3\text{--ZrO}_2$ catalyst for the selective reduction of NO by propane in the presence of excess oxygen

Olga V. Metelkina^{a,c}, Valery V. Lunin^a, Vladislav A. Sadykov^{b,*}, Galina M. Alikina^b, Rimma V. Bunina^b, Eugenii A. Paukshtis^b, Vladimir B. Fenelonov^b, Aleksandr Yu. Derevyankin^b, Vladimir I. Zaikovskii^b, Ulrich Schubert^c, and J.R.H. Ross^d

^a Physical Chemistry Department, Chemistry Faculty, Lomonosov Moscow State University, Moscow, Russia

^b Borekov Institute of Catalysis, 630090 Novosibirsk, Russia

^c Institute of Inorganic Chemistry, Vienna University of Technology, Austria

^d University of Limerick, Limerick, Ireland

Received 12 June 2001; accepted 27 September 2001

Copper catalysts supported on alumina-doped zirconia were prepared by sol–gel processing followed by supercritical drying or aging in the mother solution at 100 °C. After drying and calcination, the catalyst supports were impregnated with a copper(II) nitrate aqueous solution by the incipient wetness method to achieve a Cu loading of about 2%. The samples showed ~90% NO conversion at 350–400 °C. The catalytic performance of these systems appears to be determined by the degree of clustering of copper cations as probed by FTIR spectroscopy of adsorbed CO.

KEY WORDS: supported copper oxide; alumina-modified zirconia; sol–gel processing; NO_x selective catalytic reduction by propane

1. Introduction

During recent years zirconia has attracted much attention in heterogeneous catalysis due to its chemical and thermal stability and the simultaneous presence of both acidic and basic surface sites. However, the application of a pure zirconia as a catalyst support is limited due to the transformation of metastable tetragonal and cubic phases upon heating into the monoclinic phase which is the stable phase below 1443 K and possesses a low surface area and a poor pore structure [1,2].

The lattice of ZrO_2 can accommodate a variety of cations forming so-called partially stabilized zirconias in which the sintering and phase transition is suppressed [3]. It was also shown that alumina addition delays the crystallization, increases the specific surface area and pore volume, and enhances the surface acidity of zirconia [4,5].

High surface area mesoporous zirconia partially stabilized by alkaline-earth cations was shown to be a good support for copper cations ensuring their high performance in the selective reduction of NO_x by hydrocarbons in an excess of oxygen [6].

This paper reports the use of copper oxide supported on alumina-modified zirconia with a low crystallinity and high surface area in the selective catalytic reduction of NO_x by propane. Since copper cations clustering was earlier shown to affect the catalytic properties appreciably [6,7], FTIR of adsorbed CO was used to characterize the state of the supported copper species.

2. Experimental

2.1. Catalysts preparation

The alumina-modified zirconia supports with an alumina content 1 or 5 wt% were prepared by co-hydrolysis and co-condensation of aluminum *sec*-butoxide (97% solution in *sec*-butanol, Aldrich) and zirconium butoxide (80% solution in butanol, Aldrich) under Ar in the presence of a Pluronic block copolymer, as previously described [8]. The obtained gels were subjected to either (i) supercritical drying at 40 °C and 100 bar, using CO_2 as fluid, after solvent exchange with liquid CO_2 at 10 °C for 48 h (catalyst support 1; alumina content 1 wt%) or (ii) aging in the mother liquid (pH = 5) at 100 °C for 8 h, followed by decanting of the supernatant liquid phase (catalyst support 2; alumina content 5 wt%). After either treatment the samples were dried at 110 °C for 2 h and calcined at 500 °C for 6 h in air.

The $\text{CuO}_x/\text{Al}_2\text{O}_3\text{--ZrO}_2$ catalysts were prepared by incipient wetness impregnation of the supports with a calculated amount of an aqueous solution of $\text{Cu}(\text{NO}_3)_2$. All samples were then dried at 383 K and calcined in air at 773 K for 2 h. For comparison, a previously used $\text{CuO}_x/\text{Al}_2\text{O}_3$ catalyst [9] was prepared by impregnation of alumina (A1 type) with a specific surface 180 m^2/g (catalyst 3).

2.2. Sample characterization

Surface area and pore structure investigations were performed by nitrogen adsorption at 77 K on a Micromeritics ASAP 2010. Before measurements, each sample was degassed at 200 °C under vacuum for 4 h. The surface area and

* To whom correspondence should be addressed. E-mail: sadykov@catalysis.nsk.su

Table 1

Pore structure of copper oxide on alumina-modified zirconia samples after calcination at 500 °C

Catalyst number	Al ₂ O ₃ content (wt%)	Cu content (wt%)	S _{BET} (m ² /g)	Integral pore volume V _Σ ^a (cm ³ /g)	Mesopore surface area A _{me} ^a (m ² /g)
1	1	2	74	0.425	81
2	5	2	133	0.154	142
3	100	1	180	–	–

^a The values of the integral pore volume and mesopore surface area were calculated by the comparative method [10].

porosity data were analyzed by the BET method and the comparative method [10] (table 1), the latter being an extended modification of Sing's "α_s-method" [11] based on the comparison of the experimental adsorption isotherm with the standard isotherm measured for a nonporous or macroporous system.

XRD patterns were recorded on an automatic Philips-Goniometer PW-1050/80 powder diffractometer in the range 2θ = 10°–80° in the continuous scan mode. A graphite (002) monochromator and Cu K_α radiation (λ = 1.5406 Å) were used. The average particle size was calculated from the width of the reflections by the Debye–Scherrer equation. The profile of the reflections was approximated by a Gaussian function without correction, assuming a symmetric profile.

The ²⁷Al MAS NMR data were obtained on a Bruker DRX 400 spectrometer at 104.22 MHz. The spectra were acquired by using a 0.9 μs pulse length (equivalent to π/20 pulses measured on AlCl₃ in H₂O), 2000–3000 transients, and a 1 s relaxation delay. The spinning rate was 10 kHz. Chemical shifts were recorded relative to [Al(H₂O)₆]³⁺ as an external reference.

The surface properties of the copper catalyst species were probed by Fourier transform infrared (FTIR) spectroscopy of adsorbed CO (Bruker IFS 113V). The samples were pressed in wafers with densities 4.4–22.7 mg/cm² and pretreated in the IR cell first with 100 Torr of O₂, then in vacuum at 400 °C for 1 h. CO was adsorbed at 77 K first by introducing several doses (each CO dose corresponding to ~4 μmol), and finally setting the CO pressure to 10 Torr.

The steady-state catalytic activity for the NO reduction by propane in an excess of oxygen was determined by using 0.5–2.5 cm³ of catalyst loaded in a quartz plug-flow reactor. A standard reaction mixture comprising 10³ ppm of NO, 1.3 × 10³ ppm of C₃H₈, 10⁴ ppm of O₂ and a He balance was fed at a total flow rate of 10⁴ cm³/h, giving a gas hourly space velocity (GHSV) of 4 × 10³ h^{−1}. The analysis of the feed composition was carried out by GC.

At conversions of <50%, the effective rate constant can be calculated according to the equation of the first-order rate reaction for the plug-flow reactor, $k = -\ln(1 - X)/t$, where k is the reaction rate constant, X the conversion of NO or C₃H₈ and t is the relative contact time (cm³-catalyst/s/cm³-gas). The rates of NO reduction and propane oxidation were calculated at 350 °C by multiplication of the reaction rate

Table 2

The activation energy and specific rates of NO reduction and propane oxidation on catalyst 1 and 2 (0.1% NO + 0.13% propane + 1% O₂ in He, GHSV = 4 × 10³/h)

Catalyst	Reduction of NO		Oxidation of propane	
	E _a (kcal/mol)	W ^a × 10 ^{−14} (molec. NO/m ² s)	E _a (kcal/mol)	W ^a × 10 ^{−14} (molec. C ₃ H ₈ /m ² s)
1	20	6.0	23	3.0
2	17	2.7	17	0.6

^a W is the reaction rate calculated at 350 °C and related to the surface unit of the catalyst.

constant normalized to the surface area unit with a reagent concentration (table 2).

3. Results and discussion

3.1. Sample characterization

TEM data (not presented here) for both alumina–zirconia supports showed that they consist of agglomerated primary particles with typical sizes in the range of 5–10 nm. The surface areas were relatively high (table 1). The analysis of the nitrogen adsorption isotherms revealed that micropores are practically absent, which agrees with the close values of the S_{BET} and mesopore surface area. The porosity of sample 1 dried in the supercritical conditions is nearly three times as high as that for sample 2, while the specific surface area is twice as low. The last feature can be explained by the different content of alumina. In sample 2 with a higher aluminum content, the alumina clusters (*vide infra* NMR data) can be situated between zirconia particles thus preventing their sintering.

For both alumina–zirconia supports a broad pore size distribution without any apparent maxima or clear distinctions of pores situated in aggregates and between them was revealed. Traditional estimation of the mean mesopore sizes in the frame of the cylindrical pore model as $d_{me} = 4V_{\Sigma}/A_{me}$ gives 5.2 nm for sample 1 and 4.3 nm for sample 2. Hence, the mean size of mesopores is somewhat bigger for sample dried in the supercritical conditions.

The dried samples of catalyst supports were amorphous according to XRD investigations. After calcination, the diffraction patterns corresponded to that of the metastable tetragonal or cubic zirconia phase [12–14]. The diffraction peaks for catalyst support 2 (xerogel) were distinctly broader than that of catalyst support 1 (aerogel). From the line broadening, average zirconia particle sizes of 9.6 nm for catalyst support 1 and 4.4 nm for catalyst support 2 were calculated. No crystalline alumina phase was detected. The incorporation of alumina into zirconia thus helps to stabilize its metastable tetragonal structure at least up to 500 °C and its transition into the low-surface area monoclinic phase is prevented. No copper oxide phase (XRD) or separate copper oxide particles (TEM) were found in the copper-loaded samples annealed in air at 500 °C.

The ^{27}Al MAS NMR spectrum of catalyst support 2 showed a strong resonance at about 2 ppm typical for octahedrally coordinated aluminum, and a weaker signal at about 30 ppm, assigned to 5-coordinated Al. The spectrum was very similar to the ^{27}Al MAS NMR spectra of alumina prepared by sol-gel processing [15–17] and thus indicates that the aluminum atoms are not evenly dispersed in the zirconia matrix but instead aggregated in the form of aluminum oxide clusters. These results help to explain the difference between the surface area values of samples 1 and 2 (*vide supra*).

3.2. FTIR data

The spectral features of adsorbed CO on $\text{CuO}/\text{Al}_2\text{O}_3\text{-ZrO}_2$ differ considerably from those typical for $\text{CuO}/\text{Al}_2\text{O}_3$ with a similar amount of supported copper [18–20]. While for the latter system the band at 2145 cm^{-1} corresponding to CO complexes of flat (two-dimensional) copper oxide clusters with strongly bound bridging oxygen dominates [19], zirconia-supported copper oxidic species are characterized by a band shifted to lower ($2110\text{--}2120\text{ cm}^{-1}$) frequencies [20]. As a typical example, figure 1 demonstrates such a spectra for one of the $\text{CuO}/\text{Al}_2\text{O}_3\text{-ZrO}_2$ samples considered here. This implies that, similarly to other zirconia-supported systems [20,21], three-dimensional copper oxidic species dominate in the $\text{CuO}/\text{Al}_2\text{O}_3\text{-ZrO}_2$ samples with a reasonably high copper content. Those species are easily reduced by CO even at 77 K yielding Cu^+ cations which form strong complexes with CO [19,20]. The surface coverage of those centers by CO nearly attains saturation after 4 doses of CO. The bands in the $2150\text{--}2190\text{ cm}^{-1}$ region correspond to relatively weak CO complexes, and their intensity strongly increases with the CO dosage/pressure. The band at $\sim 2153\text{ cm}^{-1}$ corresponds to CO complexes with the surface hydroxyls [19,20]. The bands at $\sim 2176\text{--}2186\text{ cm}^{-1}$ can be assigned to CO complexes with coordinatively unsaturated Cu^{2+} cations, while a shoulder at a higher ($\sim 2195\text{ cm}^{-1}$) frequency is due to coordinatively unsaturated Zr^{4+} cations of the support [19,20].

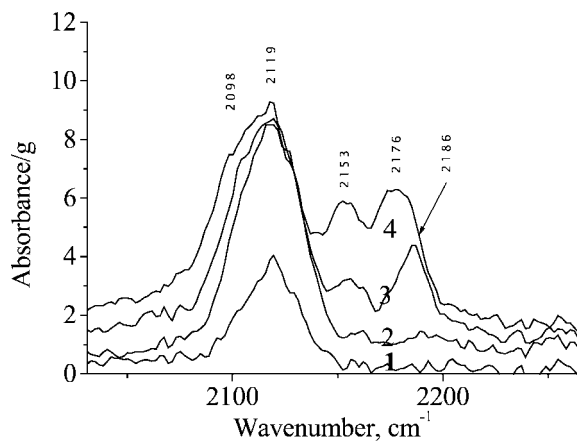


Figure 1. FTIR spectra of the catalyst 2 after adsorption of 1 (spectrum (1)), 4 (spectrum (2)) and 9 (spectrum (3)) doses of CO (each dose is equal to $4\text{ }\mu\text{mol}$) at 77 K finally setting the CO pressure to 10 Torr (spectrum (4)).

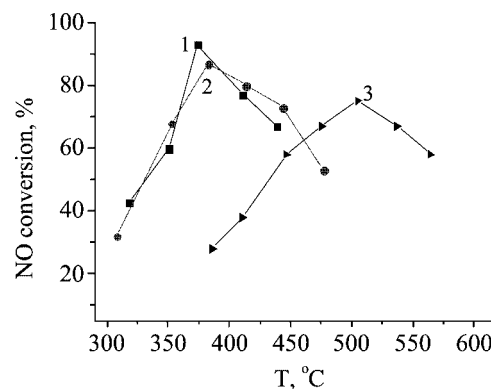


Figure 2. Temperature dependence of NO conversion into N_2 on catalyst 1 and 2, and $\text{CuO}/\text{Al}_2\text{O}_3$ (curve (3)). Reaction mixture: 0.1% NO + 0.13% propane + 1% O_2 in He, GHSV = $4 \times 10^3/\text{h}$.

3.3. Catalytic performance

The temperature dependence of the NO conversion into N_2 and the propane oxidation into CO_2 and H_2O is presented in figures 2 and 3. In no case was N_2O detected among the products. The decrease of the NO conversion after reaching a maximum at a certain temperature (T_{max}) is usually explained either by hydrocarbon depletion [7] or desorption of reactive, strongly bound nitrite–nitrate species from the surface, which are responsible for the selective reduction of NO by hydrocarbons [9,22]. For the samples discussed in the present work, the latter reason appears to be the most essential, since the propane conversion is lower than 60% at T_{max} .

The highest activity (NO conversion to N_2 about 93% at 370°C) was found for catalyst 1. This sample also shows the highest rate of propane oxidation. In the case of catalyst 2 with a higher alumina content and higher surface area, the conversion of NO is nearly unchanged (but the rate of the NO reduction is only half of that for sample 1), while the consumption of propane drops markedly (figures 2 and 3, table 2). This feature can be tentatively assigned to a lower degree of copper clustering for catalyst 2, which has a higher surface area and contains more alumina than sample 1. Incorporation of alumina into zirconia could create additional acid centers for the deposition of the copper clusters. As a matter of fact, the turnover frequency of hydrocarbons com-

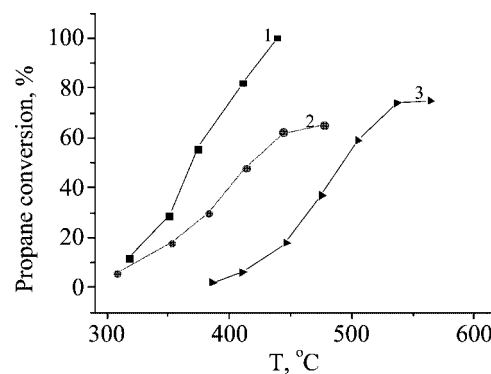


Figure 3. Temperature dependence of propane conversion into water and carbon dioxide on catalyst 1 and 2, and $\text{CuO}/\text{Al}_2\text{O}_3$ (curve (3)). Reaction mixture: 0.1% NO + 0.13% propane + 1% O_2 in He, GHSV = $4 \times 10^3/\text{h}$.

bustion for copper/zirconia catalysts usually increases with the size of copper oxidic clusters [21], which is in accordance with our results.

For comparison, copper oxide supported on alumina (figure 2, curve (3)) shows a lower maximum value of NO conversion at higher temperatures ($\sim 500^\circ\text{C}$). As follows from FTIR data (*vide supra*), this feature can be explained by the lower surface density of three-dimensional copper oxidic clusters retaining weakly bound reactive oxygen [9,20,21].

For the samples discussed in the present work, the activation energy is nearly constant and close to typical values found for the copper/alumina system [18]. Hence, the structure sensitivity observed here may be due to variation of the number of active sites. Diffusion limitations are clearly absent for all samples studied.

The most important feature of copper-supported partially stabilized zirconia samples presented in this communication is that they ensure a high (up to 90%) level of NO conversion into N_2 at rather low ($350\text{--}370^\circ\text{C}$) temperatures in the presence of an excess of oxygen using propane as reductant. Their performance approaches that of Cu-ZSM-5 with the same reductant ($\sim 100\%$ NO conversion into N_2 at $300\text{--}330^\circ\text{C}$ [18,22]). Earlier [7,23], mixed copper/zirconia samples were demonstrated to be rather active in the reaction of NO selective reduction by propylene (NO conversion up to 70% at GHSV $\sim 10^4/\text{h}$), while being only moderately active for propane as reductant (conversions not exceeding 10% at 450°C). This difference clearly implies the importance of the catalyst synthesis method affecting its microstructure.

In summary, the high performance of the samples reported in this work in the selective reduction of NO_x by propane can be explained by a higher surface coverage by copper oxide species and their higher degree of clustering. The most reactive weakly bound oxygen species are mainly located on small three-dimensional oxidic clusters, while big oxidic clusters/particles with a structure approaching that of CuO seem to be much less reactive [21,24]. Further work is aimed to find out whether decreasing of copper clustering is due to the increased alumina content or the surface properties of the support originating from different post-synthesis treatments.

4. Conclusions

Copper oxide supported on aluminum-doped zirconia prepared by sol-gel processing was demonstrated to have a high low-temperature ($\sim 350^\circ\text{C}$) performance in the selective reduction of NO by propane in the excess of oxygen, approaching that of Cu-ZSM-5. The nature of this high activity appears to stem from stabilization on the surface of alumina-modified zirconia samples of copper oxidic species with a degree of clustering close to the optimum value.

Acknowledgment

OVM thanks the Österreichischer Akademischer Austauschdienst (ÖAD), Vienna, for a scholarship. This work

was in part supported by the Fonds zur Förderung der wissenschaftlichen Forschung (FWF), Vienna, and INTAS (grant 97-11720).

References

- [1] D.A. Ward and E.I. Ko, Chem. Mater. 5 (1993) 956.
- [2] T. Klimova, M.L. Rojas, P. Castillo, R. Cuevas and J. Ramirez, Micropor. Mesopor. Mater. 20 (1998) 293.
- [3] F.C. Wu and S.C. Yu, J. Cryst. Growth 96 (1989) 96.
- [4] E. Zhao, S.E. Hardcastle, G. Pacheco, A. Garcia, A.L. Blumenfeld and J.J. Fripiat, Micropor. Mesopor. Mater. 31 (1999) 9.
- [5] Y.-W. Chen, T.-M. Yen and C. Li, J. Non-Cryst. Solids 185 (1995) 49.
- [6] V.A. Sadykov, R.V. Bunina, G.M. Alikina, V.P. Doronin, T.P. Sorokina, D.I. Kochubei, B.N. Novgorodov, E.A. Paukshtis, V.B. Fenelonov, A.Y. Derevyankin, A.S. Ivanova, V.I. Zaikovskii, T.G. Kuznetsova, S.A. Beloshapkin, V.N. Kolomiichuk, L.M. Plasova, V.A. Matyshak, G.A. Konin, A.Y. Rozovskii, V.F. Tretyakov, T.N. Burdeynaya, M.N. Davydova, J.R.H. Ross, J.P. Breen and F.C. Meunier, Mater. Res. Soc. Symp. Proc. 581 (2000) 435.
- [7] K.A. Bethke, D. Alt and M.C. Kung, Catal. Lett. 25 (1994) 37.
- [8] K.A. Bethke, C. Li, M.C. Kung, B. Yung and H.H. Kung, Catal. Lett. 31 (1995) 287.
- [9] K.A. Bethke, M.C. Kung, B. Yang, M. Shah, D. Alt, C. Li and H.H. Kung, Catal. Today 26 (1995) 169.
- [10] O. Metelkina, N. Hüsing, P. Pongratz and U. Schubert, J. Non-Cryst. Solids, in press.
- [11] V.A. Sadykov, S.L. Baron, V.A. Matyshak, G.M. Alikina, R.V. Bunina, A.Y. Rozovskii, V.V. Lunin, E.V. Lunina, A.N. Kharlanov, A.S. Ivanova and S.A. Veniaminov, Catal. Lett. 37 (1996) 157.
- [12] P. Karnauchov, V.B. Fenelonov and V.Y. Gavrilov, Pure Appl. Chem. 61 (1989) 1913.
- [13] S.J. Gregg and K.S.W. Sing, Adsorption, Surface Area and Porosity, 2nd Ed. (Academic Press, London, 1982).
- [14] S. Neeraj and C.N.R. Rao, J. Mater. Chem. 8 (1998) 1631.
- [15] M.S. Wong, D.M. Antonelli and J.Y. Ying, Nanostruct. Mater. 9 (1997) 165.
- [16] U. Ciesla, S. Schacht, G.D. Stucky, K.K. Ungner and F. Schueth, Angew. Chem. Int. Ed. Engl. 35 (1996) 541.
- [17] F. Vaudry, S. Khodabandeh and M.E. Davis, Chem. Mater. 8 (1996) 1451.
- [18] J.A. Wang, X. Bokhimi, A. Morales, O. Novaro, T. Lopez and R. Gomez, J. Phys. Chem. B 103 (1999) 299.
- [19] S. Valange, J.-L. Guth, F. Kolenda, S. Lacombe and Z. Gabelicia, Micropor. Mesopor. Mater. 35–36 (2000) 597.
- [20] O.V. Metelkina, V.V. Lunin, V.A. Sadykov, S.A. Beloshapkin, G.M. Alikina, E.V. Lunina and A.N. Kharlanov, Neftekhimika 40 (2000) 108.
- [21] S.F. Tikhov, V.A. Sadykov, G.N. Kryukova, E.A. Paukshtis, V.V. Popovskii, T.G. Starostina, V.F. Anufrienko, V.A. Razdobarov, N.N. Bulgakov and A.V. Kalinkin, J. Catal. 134 (1992) 506.
- [22] V.A. Sadykov, R.V. Bunina, G.M. Alikina, A.S. Ivanova, D.I. Kochubei, B.N. Novgorodov, E.A. Paukshtis, V.B. Fenelonov, V.I. Zaikovskii, T.G. Kuznetsova, S.A. Beloshapkin, V.N. Kolomiichuk, E.M. Moroz, V.A. Matyshak, G.A. Konin, A.Ya. Rozovskii, J.R.H. Ross and J.P. Breen, J. Catal. 200 (2001) 117.
- [23] Lj. Kundakovic and M. Flytzani-Stephanopoulos, Appl. Catal. A 171 (1998) 13.
- [24] V.A. Sadykov, S.A. Beloshapkin, E.A. Paukshtis, G.M. Alikina, D.I. Kochubei, S.P. Degtyarev, N.N. Bulgakov, S.A. Veniaminov, E.V. Netyaga, R.V. Bunina, A.N. Kharlanov, E.V. Lunina, V.V. Lunin, V.A. Matyshak and A.Ya. Rozovskii, Pol. J. Environ. Studies 1 (1997) 21.
- [25] D. Pietrogiamici, D. Sannino, S. Tuti, P. Ciambelli, V. Indovina, M. Occhiuzzi and F. Pepe, Appl. Catal. B 21 (1999) 141.
- [26] R.-X. Zhou, X.-Y. Jiang, J.-X. Mao and X.-M. Zheng, Appl. Catal. A 162 (1997) 213.